European Journal of Medicinal Chemistry 187 (2020) 111957

Contents lists available at ScienceDirect

European Journal of Medicinal Chemistry

journal homepage: http://www.elsevier.com/locate/ejmech

Research paper

Fluorine-substituted tetracationic ABAB-phthalocyanines for efficient photodynamic inactivation of Gram-positive and Gram-negative bacteria

Miguel Á. Revuelta-Maza [a], Patricia González-Jiménez [a], Cormac Hally [d], Montserrat Agut [d], Santi Nonell [d, **], Gema de la Torre [a, b, ***], Tomás Torres [a, b, c, *]

[a] Universidad Autónoma de Madrid, C/ Francisco Tomás y Valiente 7, 28049, Madrid, Spain
[b] Institute for Advanced Research in Chemical Sciences (IAdChem), Universidad Autónoma de Madrid, 28049, Madrid, Spain
[c] Instituto Madrileño de Estudios Avanzados (IMDEA)-Nanociencia, C/ Faraday 9, Cantoblanco, 28049, Madrid, Spain
[d] Institut Químic de Sarrià, Universitat Ramon Llull, 08017, Barcelona, Spain

ARTICLE INFO

Article history:
Received 11 October 2019
Received in revised form
22 November 2019
Accepted 8 December 2019
Available online 10 December 2019

Keywords:
Phthalocyanine
Cationic
Amphiphile
Photodynamic inactivation
Bacteria

ABSTRACT

Herein, we report the synthesis and characterization of new amphiphilic phthalocyanines (Pcs), the study of their singlet oxygen generation capabilities, and biological assays to determine their potential as photosensitizers for photodynamic inactivation of bacteria. In particular, Pcs with an ABAB geometry (where A and B refer to differently substituted isoindole constituents) have been synthesized. These molecules are endowed with bulky bis(trifluoromethylphenyl) groups in two facing isoindoles, which hinder aggregation and favour singlet oxygen generation, and pyridinium or alkylammonium moieties in the other two isoindoles. In particular, two water-soluble Pc derivatives (**PS-1** and **PS-2**) have proved to be efficient in the photoinactivation of *S. aureus* and *E. coli*, selected as models of Gram-positive and Gram-negative bacteria.

1. Introduction

The therapeutic properties of light have been extensively applied as a medical practice [1], yet photodynamic therapy (PDT) was principally developed in the last century. Among the therapies based on the management of light through the use of chemical substances called photosensitizers (PS), the photodynamic inactivation (PDI) of microbial cells is nowadays taking a leading position [2,3], owing to the emergence of microbial resistance to antibiotics [4]. Within this therapy, the combination of a PS, light of an appropriate wavelength, and molecular oxygen enables the generation of reactive oxygen species, such as singlet oxygen ($^1O_2$), that trigger a phototoxic cascade leading to cell death. In this context, a large variety of cationic PS have been developed and successfully tested for bacterial photo-killing [5–8]. The presence of outer positively charged terminal groups in the PS permits electrostatic interactions with the negatively charged membrane of bacteria, and therefore, facilitates their uptake by them. Phthalocyanines (Pcs), and in particular ZnPcs, are very interesting PS as they present high singlet oxygen quantum yields (Φ_Δ) [8–10]. To sort out their inherent insolubility in aqueous media, these chromophores can be endowed with hydrophilic groups [11–17]; in particular, functionalization with positively charged moieties imparts water-solubility to the Pcs and makes them potential PS in PDI [18–20]. However, owing to their extended π-conjugation, Pcs exhibit a high aggregation tendency in aqueous media, forming oligomers in solution that can be either photoactive (i.e. *J*-type aggregates) [21], or present cancelled $^1O_2$ generation abilities. Aggregation in aqueous media can be reduced by the introduction of bulky substituents in axial or peripheral positions of the Pc. Recently, our research group has described a new strategy to prepare ZnPcs presenting both water-solubility and hindered aggregation. The approach consists in introducing two types of peripheral substituents in the Pc in a

* Corresponding author. Universidad Autónoma de Madrid, C/ Francisco Tomás y Valiente 7, 28049, Madrid, Spain.
** Corresponding author. Institut Químic de Sarrià, Universitat Ramon Llull, Via Augusta 390, 08017, Barcelona, Spain.
*** Corresponding author. Universidad Autónoma de Madrid, C/ Francisco Tomás y Valiente 7, 28049, Madrid, Spain.
E-mail addresses: santi.nonell@iqs.url.edu (S. Nonell), gema.delatorre@uam.es (G. de la Torre), tomas.torres@uam.es (T. Torres).

https://doi.org/10.1016/j.ejmech.2019.111957
0223-5234/

crosswise, ABAB architecture (A and B coding for differently functionalized isoindole constituents), by using a phthalonitrile precursor (**B**) functionalized with bulky groups in the *ortho*-positions which is not able to self-condensate due to steric constrictions [22,23]. Therefore, these molecules hold two facing isoindoles endowed with bulky bis(trifluoromethylphenyl) moieties that avoid the aggregation in solution, and other two that can be functionalized with substituents that render water-solubility to the molecule. Furthermore, we have recently demonstrated that the functionalization with trifluoromethylphenyl units at the B units of ABAB ZnPcs gives rise to high Φ_Δ [24,25].

Taking advantage of this successful design, the objective of the present work is to synthesize and characterize new ZnPcs with potential use as PS for PDI, by incorporating hydrophilic cationic-terminated substituents in the A isoindole that provide these ABAB ZnPcs with solubility in aqueous media. *In vitro* assays with two selected ZnPcs (**PS-1** and **PS-2**) have been performed to examine their toxicity in different bacterial strains and their potential and efficiency as PS for PDI.

2. Results and discussion

2.1. Synthesis

Two different functionalization approaches have been undertaken to perform the preparation of amphiphilic tetracationic ABAB ZnPcs, namely the functionalization with either pyridines or tertiary amines, which could be quaternized in a final step (Scheme 1). The aim is to compare the effect of the nature of the positively charged groups and/or the bridge between the positive charge and the aromatic core on their activity as PS. The synthesis of phthalonitrile **B** was carried out following the methodology described in our group [22]. The preparation of ZnPcs functionalized with pyridine units was undertaken by two different synthetic approaches. First, we prepared the already described ZnPcs **1** [22] and subjected it to a four-fold Sonogashira coupling with 4-ethynylpyridine, yielding **5**. Although the product was isolated and fully characterized, the low yield of this reaction (11%), preceded by the 10% yield of the mixed cyclotetramerization between **A-1** and **B**, which makes and overall yield of 1%, made us discard this route as an operative method to obtain pyridine functionalized PS for *in vitro* assays. Therefore, we prepared **2**, resulting from the straightforward cross-condensation between bulky phthalonitrile **B** and **A-2** (Scheme 1). Although the cross-condensation yield was low (8%), **2** was easily purified, and the pyridyl moieties could be easily quaternized by reaction with MeI. In a last step, the compound was exposed to Dowex® resin in order to exchange the initial counterions for chloride anions, rendering a compound that was partially soluble in water, from now coded as **PS-1** for the photophysical characterization and further *in vitro* experiments.

Moving to the preparation of ABAB ZnPcs functionalized with alkyl ammonium moieties, we intended to explore the preparation of a series of compounds with different separation between the aromatic core and the positive charges. The first tailored ABAB ZnPc derivative was compound **3**, in which the tertiary amines were separated from the ZnPc core by a $(CH_2)_2$—S- bridge. Since alkyl thioether chains can be easily introduced in the starting phthalonitriles by aromatic nucleophilic substitution over 4,5-dichlorophthalonitrile [26], phthalonitrile **A-3** was synthesized and reacted with phthalonitrile **B** under the typical conditions applied for the preparation of ABAB ZnPc derivatives. Worth mentioning, the reaction proceeded in 20% yield, proving this conversion as one of the most efficient cross-condensation reactions performed between bulky phthalonitrile **B** and another differently substituted phthalonitrile performed to date. **3** was then

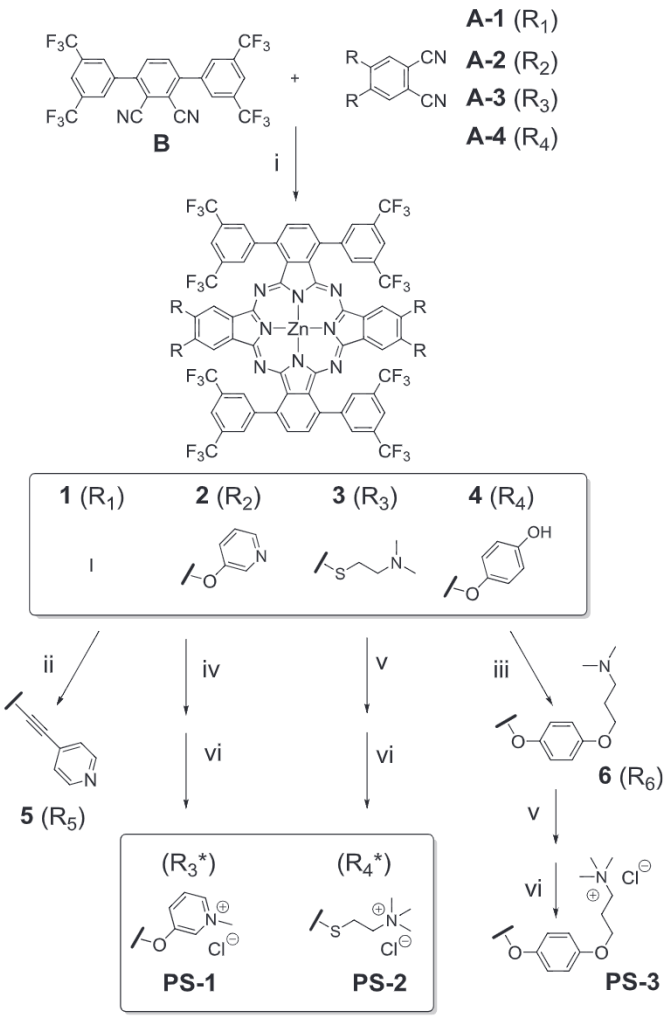

Scheme 1. Synthesis of pyridil or alkylamino-substituted ZnPcs and their respective pyridinium and ammonium salts. i) $Zn(OAc)_2$, *o*-DCB/DMF (2:1), 150 °C, overnight; ii) 4-ethynylpyridine, $PdCl_2(PPh_3)_2$, CuI, diisopropylamine, 70 °C, overnight; iii) 3-(dimethylamino)propyl methyl carbonate, CH_3CN, 180 °C, MW, 90 min; iv) MeI, DMF, 4 h; v) MeI, EtOH, reflux, overnight; vi) Dowex® (1x8 200–400), MiliQ water, DMSO.

methylated with MeI in dry EtOH, in 36% yield. Noteworthy, after this transformation, the solubility of the resulting product changed drastically, becoming soluble only in polar solvents such as DMSO or DMF. In a last step, the product was exposed to Dowex® resin for ionic exchange, thus yielding a compound soluble in water. From now this product will be coded as **PS-2** for the photophysical characterization and *in vitro* tests. Our second approach towards an alkyl-ammonium functionalized ZnPc was to increase the distance between the ZnPc and the positive charge by preparing compound **4**, which was consecutively subjected to a four-fold *O*-alkylation to introduce *N*-dimethylamino-*N*-propyl residues. In particular, we performed the *O*-alkylation by heating at 180 °C a mixture of **4** and excess of 3-(dimethylamino)propyl methyl carbonate [27] in acetonitrile. The formation of **6** was efficient, namely, 11% yield starting from the mixture of **A-4** and **B** phthalonitriles). **6** was then subjected to a methylation reaction, and further exposed to Dowex® resin to exchange the initial iodides for chloride anions. Unfortunately, this compound, coded as **PS-3** in Scheme 1, proved unstable in solution, undergoing Hoffman-type eliminations of the alkylammonium moieties that lead to molecules with terminal double bonds in the peripheral alkyl chains, as detected by mass spectrometry. This chemical instability made us discard **PS-3** for

in vitro assays.

Fig. 1 shows the ^{1}H NMR spectra of **PS-1** and **PS-2**. In both cases, the signals are well resolved due to their non-aggregated state in DMSO-d_6 solutions. The reduced number of signals derives from the high molecular symmetry these compounds possess (i.e. D_{2h}). In the case of **PS-1**, the spectrum presents four singlets for the aromatic protons of the isoindole units and the CF_3-substituted phenyl rings, a group of signals corresponding to the *ortho* substituted pyridines (two doublets, a doublet of doublets and one singlet), and one singlet for the methyl groups. In the case of **PS-2**, the distinctive signals of this product (i.e. the two triplets for the methylenes) appear overlapped with the DMSO signal, but the singlet corresponding to the methyl groups of the tertiary amines could be clearly observed. Moreover, HR-MS characterization confirmed the structure of the compounds.

2.2. Photophysical characterization

Table 1 presents a summary of the photophysical properties of **PS-1** and **PS-2** in methanol, including molar absorption coefficients (ε), wavelength, lifetime (τ_S) and quantum yield of fluorescence emission (Φ_F), and singlet oxygen quantum yield (Φ_Δ), while the photophysical data for ZnPcs **1**–**6** in included in the Supporting Information (Fig. S2). The absorption spectra of **PS-1** and **PS-2** (see Fig. 2 for the UV–vis spectra in MeOH) show symmetric, non-split *Q*-bands, which is not usual for MPcs with D_{2h}-symmetry. The tioeher-derivatized Pc (**PS-2**) shows a *Q*-band more shifted to the red than the ether-derivatized one (**PS-1**), and with a higher absorption coefficient. Indeed, the absorption spectra of these compounds in MeOH do not show any evidence of aggregation, as otherwise expected for these compounds due to the presence of rather bulky substituents at the non-peripheral positions of the Pc core. Absorption spectra were registered in a range of concentrations (between 8.7 x 10^{-7} M and 4.1 x 10^{-6} M for **PS-1**, and 1.6 x 10^{-6} M and 4.9 x 10^{-6} M for **PS-2**) (Fig. S3). For the verification of the Lambert-Beer law, an analysis of linear regression between the intensity of the *Q*-band and the concentration was performed, with

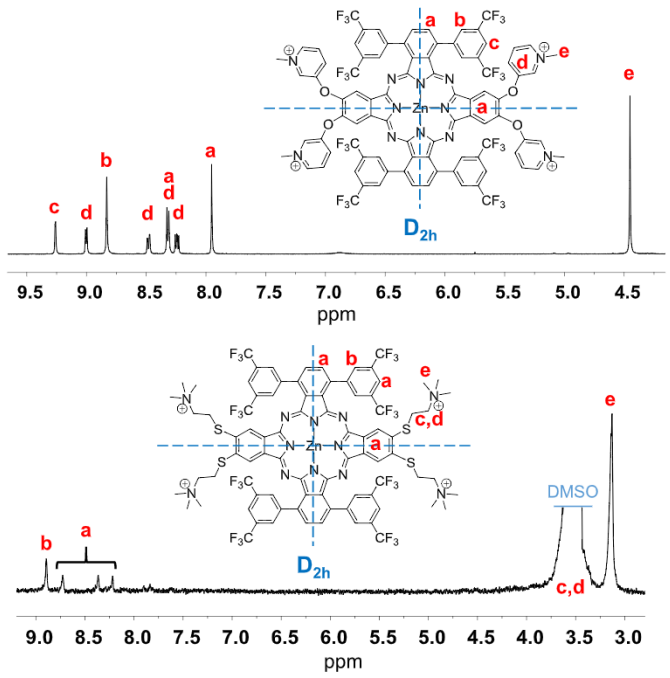

Fig. 1. ^{1}H NMR in DMSO-d_6 of **PS-1** (up); and **PS-2** (down).

Table 1
Photophysical properties of **PS-1** and **PS-2** in MeOH.

Sample	Solvent	logε (λ)*: max	λ_F/nm	Φ_F	τ_S/ns	Φ_Δ
PS-1	MeOH	4.59 (350), 5.13 (678)*	683	0.13	2.7	0.49
PS-2	MeOH	4.74 (359), 5.20 (694)*	699	0.11	2.4	0.35

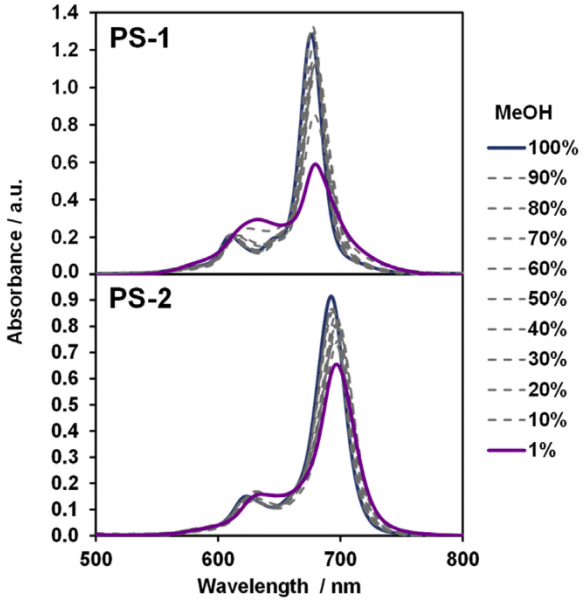

Fig. 2. Aggregation tendency upon increasing water percentage over **PS-1** and **PS-2** solutions in MeOH at constant concentration of the PS in the range: 6–9·10^{-6} M.

R^2 values of ~0.999. Fluorescence studies (Table 1 and Fig. S4) that were also performed in MeOH are in line with absorption assays; the monoexponential fluorescence decay kinetics confirm that **PS-1** and **PS-2** are in monomeric form in solution. Also, the quantification of the Φ_Δ was performed for these compounds, by direct observation of the $^1O_2$ phosphorescence at 1275 nm after excitation at 355 nm (Fig. S5). The values of Φ_F and τ_S are similar for the two compounds, however **PS-2** shows a lower Φ_Δ than **PS-1**. These results point to an enhanced internal conversion in **PS-2**, which is consistent with the higher flexibility of its structure. Comparing the photophysical parameters of **PS-1** with those of a neutral ZnPc described previously with a similar functionalization (i.e. 4-methoxyphenoxy moieties) [25], τ_S of **PS-1** is 50% longer, its Φ_F has almost doubled and its Φ_Δ has decreased by 42%, which indicate a decrease in the intersystem-crossing rate constant, probably due to the presence of the positive charges. Still, the values are adequate for phototherapeutic applications. Importantly, we tried to perform measurements of $^1O_2$ generation in water, but only residual signals were detected, which can be rationalized by the formation of aggregates, which is not fully hindered for these PS in aqueous media (see below).

2.3. Aggregation studies and determination of the log $P_{O/W}$

In addition to the photophysical and photochemical characterization, some aggregation studies are also needed to evaluate the possible application of our ABAB ZnPcs as potential PS. Due to the hydrophobic nature of the Pc ring, these chromophores have tendency to form aggregates in solution to minimize the solvation energy, particularly in the case of polar solvents as water. Aggregation is a complex process that depends on the van der Waals

interaction, π−π stacking, concentration and the environment characteristics. Although a certain organization of the PS in vesicles or micelles can facilitate their transport through the blood system, it is important that once the PS are delivered to the target cell they stay as non-aggregated species, at least to some extent, leading to a more efficient $^1O_2$ generation after light excitation. For that reason, aggregation studies in aqueous media are fundamental for the former evaluation of the potential PS. These studies are usually performed by means of UV−vis studies. As mentioned above, **PS-2** is soluble in pure water, but not **PS-1**, although it happens to be soluble upon addition of a stock of polar organic solvent solution, such as MeOH or DMSO, to water. In fact, **PS-1** remained soluble until a 99:1 water/organic solvent ratio was reached. Therefore, we performed aggregation studies by progressively adding water to MeOH solutions of **PS-1** and **PS-2**, keeping the concentration constant (Fig. 2). Upon the addition of water, the two compounds showed a similar behaviour that is a decrease in the intensity of the *Q*-band and a slight red shift and broadening. While **PS-2** proved only slightly aggregated in MeOH/water 99:1 solution, a much more pronounced aggregation was observed for **PS-1,** due to the larger hydrophobic nature of the pyridine rings compared to the alkyl amines of **PS-2**.

In order to compare the aggregation behaviour of both PS in physiologically relevant medium, that is phosphate buffered saline (PBS), concentration-dependent UV−vis studies were performed (Fig. 3). The solutions were prepared starting from stock solutions in DMSO, following the same protocol than will be further used for dosing the PS to bacteria.

Although the recorded spectra resemble those typical of non-aggregated Pcs, the relative intensity of the *Q*-band for **PS-1** (at 681 nm), and for **PS-2** (at 695 nm) with respect to their respective shoulder at 650 nm is very from that of molecularly dissolved Pcs. Moreover, while a Beer-Lambert plot is apparently linear (Fig. S6), the slope yields values of $\log(\varepsilon/cm^{-1}\cdot M^{-1}) = 4.7$ for both PS, which are one order of magnitude lower than in methanol. Also the intercept is negative for both PS, which suggests a curve with upward-deviation from linearity. Indeed, a much better fit can be obtained by using the monomer-dimer equilibrium model equation [28], indicating that the dimer absorbs more than two monomers. Data reduction yields the absorption coefficients for the monomer and the dimer, and the equilibrium constant for dimerization (*K*) (Table 2). Formation of aggregates is consistent with the almost complete inhibition of $^1O_2$ production in water.

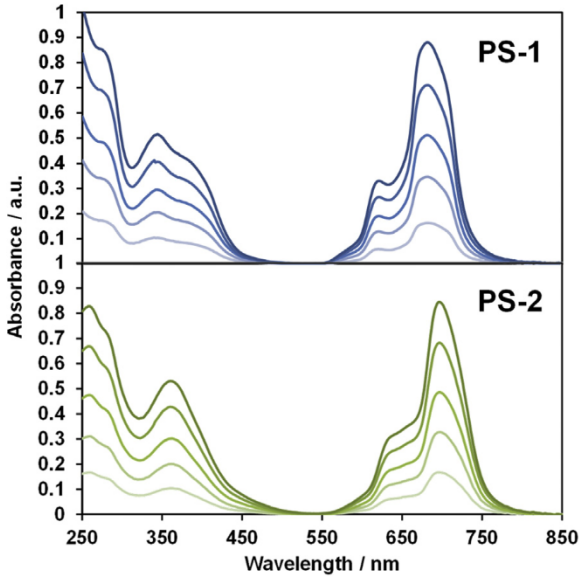

Fig. 3. Aggregation study in PBS (from stock solution in DMSO <2%), for **PS-1** and **PS-2** (concentration range from ≈3 x10^{-6} to 2 x10^{-5} M).

Photodynamic efficiency depends also on lipophilicity, which has been recognized as a factor that can determine cellular uptake, and consequently, the phototoxicity of PSs [29,30]. The affinity of a compound for cell membranes may be numerically represented by its membrane-water partition coefficient, that is, the membrane-water concentration ratio. As this value is usually difficult to measure, the *n*-octanol/PBS partition coefficient ($P_{O/W}$) is a useful quantitative parameter for evaluating the lipophilic/hydrophilic balance, and has been extensively utilized to predict the relative tendency of drugs to interact or incorporate in biological membranes [31−33]. To evaluate the affinity of **PS-1** and **PS-2** for cell membranes, and the relative lipophilicity of the compounds, the *n*-octanol/PBS partition coefficient for each Pc was determined using the shake-flask method (see Supporting Information), which does not require standard compounds and is based on the direct determination of equilibrium partition concentrations of a compound in a biphasic system. Although both compounds have a common structural core, they exhibited different amphiphilic character. **PS-1** renders a higher octanol/water partition coefficient than **PS-2** (see Table 2), indicating that the former has a more lipophilic nature. In fact, the Pc concentration reached for **PS-1** in n-octanol was approximately 200 times higher than in PBS, while the **PS-2** concentration was only 5−6 times higher in *n*-octanol than in PBS. Therefore, the log $P_{O/W}$ values suggest that **PS-1** is mostly hydrophobic and have very high affinity for membranes. Nevertheless, **PS-2** is more amphiphilic and its presence in the aqueous phase is bigger, which is concomitant which its higher solubility in this medium.

2.4. Photodynamic inactivation studies

The photodynamic studies were performed testing **PS-1** and **PS-2** in *S. aureus* and *E. coli* bacteria, chosen as models for Gram-positive and Gram-negative bacteria, respectively (Fig. 4). The inactivation studies present a typical light- and concentration-dependent profile. **PS-1** and **PS-2** were able to induce 99.9% (3 log decrease in colony-forming units, CFUs) of *S. aureus* inactivation at 0.1 and 0.5 μM, respectively, using a red light fluence of 33 J·cm^{-2}. This observation indicates that the ZnPcs must be in monomeric, i.e., photochemically active, form, which in turn indicates that they are bound to the bacterial cell wall, where they deaggregate [34]. Reducing the light fluence to 11 J·cm^{-2} only resulted in a cell survival increase of 1 log CFU. Full inactivation (7 log CFUs) could be achieved at 10 μM for both **PS-1** and **PS-2**, even though 4-logs can be attributed to dark cytotoxicity at such high concentration. Regarding *E. coli,* larger concentrations were required to induce a comparable cell death. Up to 50 μM of either PS was needed to completely inactivate the bacterial strain, whilst 10 μM and 33 J·cm^{-2} were enough to achieve a disinfection (99.9%) status. In this case, no dark toxicity could be observed even at the highest concentration, which likely indicates that the compounds are not taken up by the bacteria but stick to the outer membrane [35]. This confirms that Gram-negative bacteria are harder to photo-inactivate by PDT than Gram-positive ones, an observation that has been thoroughly described in the literature [36]. The reason behind this difference is found in the composition of the bacterial wall. Importantly, there are no dramatic differences in activity between **PS-1** and **PS-2** against the microbial strains tested, indicating a minor effect of the nature of the cationic moieties, as observed previously by Ruiz-Gonzalez and co-workers for two related porphycene macrocycles [37]. Compared to other symmetrically-substituted cationic Pcs, the bulky

Table 2
Photophysical properties and log $P_{O/W}$ of **PS-1** and **PS-2** in PBS.

Sample	$\varepsilon(m^{a})^{[a]}/M^{-1}\cdot cm^{-1}$	$\varepsilon(m^{a})^{[b]}/M^{-1}\cdot cm^{-1}$	$\varepsilon(d^{**})^{[b]}/M^{-1}\cdot cm^{-1}$	K	log $P_{O/W}$
PS-1	50110	24181	106290	$1.1\cdot10^{6}$	2.33
PS-2	53818	48422	107351	$7.5\cdot10^{5}$	0.73

[a] m: monomer; **d: dimer; [a] Beer Lambert; [b] Lavenberg-Marquardt.

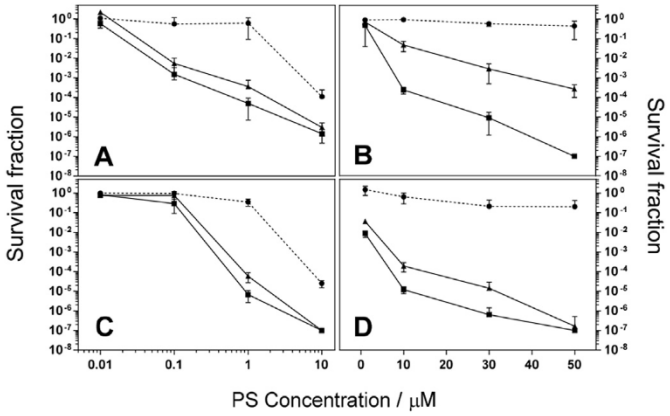

Fig. 4. Survival curves of *S. aureus* (A, C) and *E. coli* (B, D) with **PS-1** (A, B) and **PS-2** (C, D) after PDI treatment. Circles, triangles and squares represent 0 (dark toxicity), 11 and 33 $J\cdot cm^{-2}$, respectively.

bis(trifluoromethylphenyl) groups attached to **PS-1** and **PS-2** provide them with much stronger photo-antimicrobial activity. Indeed, related Pcs lacking these groups achieved only a modest 1-2-log CFUs cell death, owing to their strong aggregation [38,39]. This issue has now been solved by constructing asymmetric compounds with large steric hindrance that alleviate the aggregation problems.

3. Conclusions

Two different cationic ABAB-ZnPcs (**PS-1** and **PS-2**) have been synthesized as PS for PDI. The peculiar functionalization of these Pcs with facing bulky substituents that provide the molecules with hampered aggregation and lipophilicity, and facing hydrophilic pyridinium (**PS-1**) or alkylamonium (**PS-2**) moieties that impart water-solubility, makes these molecules suitable candidates for the inactivation of bacteria. In order to probe the validity of the design, photophysical evaluation of their $^{1}O_2$ generation capabilities, as well as aggregation assays, have been carried out with **PS-1** and **PS-2**. Non-aggregated MeOH solutions of both PS efficiently generate $^{1}O_2$, but only residual signals were detected in water, which can be rationalized by a certain degree of aggregation. In fact, UV–vis experiments in aqueous media indicate that both PS form aggregates at some extent. Nevertheless, *in vitro* photodynamic assays carried out over *E. coli* and *S. aureus* show that they are photochemically active, inducing bacteria inactivation under red light irradiation, which in turn indicates that they are bound to the bacterial cell wall, where they de-aggregate. It has been proved that **PS-1** and **PS-2** are not toxic for bacteria in darkness in the selected range of concentrations, but when the colonies are irradiated a high fatality turns out. In this regard, there is a minor effect of the nature of the cationic moieties on the activity of these PS. Nevertheless, an important conclusion is that these cationic PS have proved much stronger activity than other related cationic Pcs as a result of the rational design that has rendered improved oxygen generation abilities [25], well-balanced lipophilicity/hydrophilicity and diminished aggregation issues.

4. Experimental section

4.1. General methods and characterization techniques

Chemical reagents were purchased from Merck-Sigma Aldrich, Alfa Aesar, Acros Organics, TCI or Fluorochem, as main commercial suppliers, and were used without further purification unless it is indicated. Solvents were purchased from Carlo Erba Reagents, and anhydrous solvents were dried with 4 Å molecular sieves (Panreac). The monitoring of the reactions has been carried out by thin layer chromatography (TLC), employing aluminium sheets coated with silica gel type 60 F254 (0.2 mm thick, E. Merck). Purification and separation of the synthesized products was performed by column chromatography, using silica gel (230–400 mesh, 0.040–0.063 mm, Merck). Gel permeation chromatography (GPC) was performed using Bio-Beads S-X1 (200–400 mesh, Bio-Rad). Microwave (MW) reactions were carried out in a Biotage Initiator +4.1.2, in closed glass vials (Biotage 2–5 mL, 0.2–0.5 mL) under argon atmosphere. Aggregation studies were performed using aqueous MiliQ water or phosphate-buffered saline solution (PBS), and organic solvents. Infrared (IR) spectra were recorded on a Cry 630 FTIR spectrophotometer from Agilent Technologies, using solid samples (diamond ATR). Mass spectrometry (MS) and high resolution MS (HR-MS) were recorded using positive ESI Positive TOF_MS or Matrix-Assisted Laser Desorption/Ionization (MALDI). MALDI-TOF MS and high-resolution (HR-MS) mass spectra were recorded with a Bruker Ultrareflex III spectrometer. Electrospray Ionization (ESI) mass spectra were recorded with an API Q-Star Pulsar i from Sciex. Matrix used are indicated in each spectrum. MS data are expressed in *m/z* units. All MS experiments were carried out at the Servicio Interdepartmental de Investigación (SIdI) of the Universidad Autónoma de Madrid. Nuclear magnetic resonance spectra (^{1}H NMR and ^{13}C NMR) were recorded on Bruker AC-300 (300 MHz) or Bruker XRD-500 (500 MHz) instruments. Deuterated solvents employed are indicated in each spectrum. UV–vis spectra were recorded with a UV–vis JASCO-V660 spectrophotometer using spectroscopy grade solvents and 10 × 10mm quartz cuvettes for aggregation experiments.

4.2. Synthesis

Compounds 3,3″,5,5″-tetrakis(trifluoromethyl)-[1,1′:4′,1″-terphenyl]-2′,3′-dicarbonitrile (**B**) [22], 4,5-diiodophthalonitrile (**A-1**) [40], 4,5-bis(pyridin-3-yloxy)phthalonitrile (**A-2**) [41], 4,5-bis(4-hidroxiphenoxy)phthalonitrile (**A-3**) [42], 4,5-bis[(2-(dimethylamino)ethyl)thio]phthalonitrile (**A-4**) [26], ZnPc **1** [22], 4-ethinylpyridine [43], and 3-(dimethylamino)propyl methyl carbonate (**8**) [44], were prepared according to previously reported procedures.

ZnPc **2:** Phthalonitrile **B** (149 mg, 0.27 mmol), phthalonitrile **A-2** (1 eq) and anhydrous $Zn(OAc)_2$ (1 eq) were placed in a 5 mL high pressure resistant flask equipped with a magnetic stirrer, and then 2.7 mL ([**B**] = 0.1 M) of dry *o*-DCB/DMF 2:1 were added. The mixture was heated to 150-160 °C overnight under an argon atmosphere. After cooling the solvent was removed under vacuum. The product was purified by column chromatography on SiO_2 (heptane/EtOAc

1:3 with 1% pyridine) where the second blue-green fraction to elute containing the desired product **2**. A second batch of the product that was strongly retained can be eluted from the column using THF:pyridine (7:1). After evaporation of the solvent a blue-green solid was obtained, which was precipitated from MeOH with water. Yield: 18.8 mg (8%). ^{1}H NMR (300 MHz, THF-d_8): δ 8.75 (s, 8H, Ar), 8.41 (dd, J = 11.15 Hz, J = 2.76 Hz, 8H, Ar-py), 8.23 (s, 4H, Ar), 8.10 (s, 4H, Ar), 8.03 (s, 4H, Ar), 7.46–7.31 (m, 8H, Ar-py); ^{13}C NMR (125 MHz, DMSO-d_6): δ 120.1, 123.4, 124.5, 124.7, 130.5, 131.2, 134.8, 136.1, 139.7, 142.4, 144.1, 144.8, 147.9, 148.7, 149.8, 151.7, 152.5, 153.7; IR(ATR) ν^{-1} (cm^{-1}): 2920, 2851, 1592, 1458, 1377, 1275, 1132. HR-MS (MALDI, matrix DCTB + PMMANa 2100 + NaI) for $C_{84}H_{36}F_{24}N_{12}O_4Zn$: *m/z* 1796.1857 [M$^+$] (calculated: 1796.1885).

PS-1: 2 (10 mg, 5.56·10^{-3} mmol) was placed in a 10 mL round bottom flask equipped with a magnetic stirrer and 1 mL of dry DMF (dried over 4 Å molecular sieves) were added. Then, an excess of MeI (150 μL) was added and the mixture was stirred at room temperature for 4 h under argon atmosphere. Then 10 mL of diethylether were added and the product was collected by filtration and washed several times with diethylether as a blue solid. Yield: 8.0 mg (61%). 250 mg of Dowex® (1x8 200–400) were suspended in 10 mL of MiliQ water, the product was previously dissolved in 0.2 mL of DMSO was added and stirred for 2 h. Then, the mixture was filtered, washed with diethylether, and evaporated under vacuum. ^{1}H NMR (500 MHz, DMSO-d_6): δ 9.26 (s, 4H, Ar), 9.00 (d, J^1 = 6.00 Hz, 4H, Ar-py), 8.83 (s, 8H, Ar), 8.48 (d, J^2 = 8.87 Hz, 4H, Ar-py), 8.33 (s, 4H, Ar), 8.31 (s, 4H, Ar-py), 8.24 (dd, J^2 = 8.87 Hz, J^1 = 6.00 Hz, 4H, Ar-py), 7.95 (s, 4H, Ar), 4.45 (s, 12H, Me); IR (ATR) ν^{-1} (cm^{-1}): 3016, 2931, 1584, 1498, 1409, 1276, 1171, 1125. HR-MS (ESI Positive TOF_MS-100-3500.m) for $C_{88}H_{48}F_{24}N_{12}O_4Zn$: *m/z* 630.4153 [MCl]$^{3+}$ (calculated: 630.4167); 963.1093 [MCl$_2$]$^{2+}$ (calculated: 963.1098).

ZnPc **3:** Phthalonitrile **B** (149 mg, 0.27 mmol), phthalonitrile **A-3** (1 eq) and anhydrous Zn(AcO)$_2$ (1 eq) were placed in a 5 mL high pressure resistant flask equipped with a magnetic stirrer, and then 2.7 mL ([**B**] = 0.1 M) of dry *o*-DCB/DMF 2:1 were added. The mixture was heated to 150-160 °C overnight under an argon atmosphere. After cooling the solvent was removed under vacuum. The product was purified by column chromatography on Bio-Beads using $CHCl_3$ as eluent. After evaporation of the solvent a blue solid was obtained, which was washed with heptane. Yield: 50 mg (20%). ^{1}H NMR (300 MHz, THF-d_8): δ 2.35 (s, 24H, NMe_2); 2.81 (t, J = 7.09 Hz, 8H, CH_2); 3.23 (t, J = 7.09 Hz, 8H, CH_2); 8.12 (s, 4H, Ar); 8.24 (s, 4H, Ar); 8.58 (s, 4H, Ar); 8.84 (s, 8H, Ar). ^{13}C NMR (75 MHz, THF-d_8): δ 33.4 (CH_2), 45.6 (NMe_2), 58.7 (CH_2), 122.4, 122.8 (brs, C*CF_3), 125.0 (q, J = 272.42 Hz, CF_3), 132.1, 132.4, 132.8, 136.4, 136.9, 137.9, 142.0, 144.3, 153.4, 154.4 (C=N). IR (ATR) ν^{-1} (cm^{-1}): 2930 (ar, C–H st), 1729, 1668, 1380 (pyrrole ring), 1279, 1179 (C–F st), 1134 (C–F st). HR-MS (MALDI, matrix: DCTB + PMMA 2100 + NaI) for $C_{80}H_{60}F_{24}N_{12}S_4Zn$: *m/z* 1837.2917 [M+H]$^+$ (calculated: 1837.2928).

PS-2: 3 (33 mg, 0.01769 mmol) was placed in a 5 mL high pressure resistant flask equipped with a magnetic stirrer and 0.9 mL of dry EtOH (dried over 4 Å molecular sieves) were added. Then, an excess of IMe (20 eq) was added and the mixture was refluxed overnight. After cooling the solvent was removed under vacuum. The residue was washed with $CHCl_3$, heptane, diethylether and $CHCl_3$ again, and a green solid was obtained. Yield: 13 mg (36%). 250 mg of Dowex® (1x8 200–400) were suspended in 10 mL of MiliQ water, the product was dissolved in 0.2 mL of DMSO was added and stirred for 2 h. Then, the mixture was filtered, washed with diethylether, and evaporated under vacuum. ^{1}H NMR (300 MHz, DMSO-d_6): δ 3.13 (s, 36H, NMe_3); 8.22 (s, 4H, CHAr); 8.36 (s, 4H, CHAr); 8.73 (s, 4H, CHAr); 8.89 (s, 8H, CHAr); CH_2 signals are overlapped by the solvent. IR (ATR) ν^{-1} (cm^{-1}): 2929 (ar, C–H st), 1682, 1482, 1388 (pyrrole ring), 1278, 1179 (C–F st), 1132 (C–F st). HR-MS (ESI Positive TOF_MS-50-3000.m) for $C_{84}H_{72}F_{24}N_{12}S_4Zn$: *m/z* 474.0942 [M]$^{4+}$ (calculated: 474.0943); 643.7829 [MCl]$^{3+}$ (calculated: 643.7822); 983.1589 [MCl$_2$]$^{2+}$ (calculated: 983.1580).

ZnPc **4:** Phthalonitrile **B** (149 mg, 0.27 mmol), phthalonitrile **A-4** (1 eq) and anhydrous Zn(AcO)$_2$ (1 eq) were placed in a 5 mL high pressure resistant flask equipped with a magnetic stirrer, and then 2.7 mL ([**B**] = 0.1 M) of dry *o*-DCB/DMF 2:1 were added. The mixture was heated to 150-160 °C overnight under an argon atmosphere. After cooling the solvent was removed under vacuum. The product was purified by column chromatography on SiO_2 (dioxane/heptane in gradient from 1:1 to 2:1) where the first fraction to elute containing the desired ABAB-ZnPc **4**. The product was further purified by an additional column chromatography on Bio-Beads using $CHCl_3$ as eluent. After evaporation of the solvent, a blue solid was obtained, which were recrystallized from DCM/heptane. Yield: 43 mg, (17%). ^{1}H NMR (300 MHz, DMSO-d_6): δ 6.84 (d, J = 8.72 Hz, 8H, O-Ph-O); 6.98 (d, J = 8.72 Hz, 8H, O-Ph-O); 7.72 (s, 4H, CHAr); 8.03 (s, 4H, CHAr); 8.23 (s, 4H, CHAr); 8.77 (s, 8H, CHAr); 9.33 (s, 4H, OH). ^{13}C NMR (75 MHz, DMSO-d_6): δ 116.1, 118.7, 125.2, 129.8, 130.3, 131.1, 132.1, 133.6, 134.6, 136.0, 136.9, 142.3, 147.1, 149.7, 150.8, 152.1, 153.6; IR (ATR) ν^{-1} (cm^{-1}): 3392 (O–H st), 2924 (ar, C–H st), 1505, 1411, 1378 (pyrrole ring), 1277 (C–O–C st as), 1196 (C–F st), 1181 (O–H δ ip), 1134 (C–F st); HR-MS (MALDI, matrix: DCTB) for $C_{88}H_{40}F_{24}N_8O_8Zn$: *m/z* 1856.1870 (calculated: 1856.1872).

ZnPc **5: 1** (15 mg, 8.2 x 10^{-3} mmol), **7** (6.67 eq), $PdCl_2(PPh_3)_2$ (0.040 eq) and CuI (0.040 eq), were dissolved in 1 mL of dry diisopropylamine (distilled with CaH_2 and collected over 4 Å activated molecular sieves) and stirred at 70 °C overnight under argon atmosphere. The mixture was diluted with chloroform (20 mL) and washed with water (3x20 mL), dried over $MgSO_4$, filtrated and evaporated under vacuum. The product was purified by column in Bio-Beads using chloroform as eluent, and then by column chromatography on SiO_2 (EtOAc/pyridine 99:1 and then THF/pyridine) being the product the last eluted fraction. After evaporation the green solid was washed with heptane. Yield: 1.5 mg (11%). ^{1}H NMR (300 MHz, THF-d_8): δ 7.67 (d, J = 5.76 Hz, 8H, py), 8.34 (s, 4H, Ar), 8.45 (s, 4H, Ar), 8.63 (s, 4H, Ar), 8.72 (d, J = 5.76 Hz, 8H, py), 8.85 (s, 8H, Ar). ^{13}C NMR: The low amount obtained due to the low yield prevented obtaining the spectrum. IR (ATR) ν^{-1} (cm^{-1}): 2959, 2927, 2359, 1591, 1377, 1275, 1165, 1132. HR-MS (MALDI (ULTRAFLEX III) DCTB + PEGNa 2000) for $C_{92}H_{36}F_{24}N_{12}Zn$: *m/z* 1828.2112 [M]$^+$ (calculated: 1828.2089).

ZnPc **6: 4** (15 mg, 0.008 mmol) and **8** (15.6 mg, 0.09 mmol) were placed in a 5 mL high pressure resistant flask equipped with a magnetic stirrer and 0.85 mL of dry acetonitrile were added. Solution was heated for 90 min at 180 °C under MW irradiation. After cooling, the mixture was transferred into a flask and the solvent evaporated to dryness. Finally, product was poured onto heptane and the resulting green precipitate was filtered off and dried over vacuum. Yield: 11 mg (62%). ^{1}H NMR (500 MHz, DMSO-d_6): δ 1.91 (t, J = 6.52 Hz, 8H, CH_2), 2.19 (s, 24H, CH_3), 2.45 (m, 8H, CH_2), 4.03 (t, J = 6.45H, 8H, CH_2), 7.02 (d, J = 8.34 Hz, 8H, Ar), 7.06 (d, J = 8.34 Hz, 8H, Ar), 7.75 (s, 4H, Ar), 7.97 (s, 4H, Ar), 8.23 (s, 4H, Ar), 8.77 (s, 8H, Ar). ^{13}C NMR (125 MHz, DMSO-d_6): δ 26.9, 45.1, 55.8, 66.3, 115.5, 115.7, 116.1, 118.5, 122.4, 129.9, 130.2, 131.2, 132.1, 134.6, 136.0, 152.2. IR (ATR) ν^{-1} (cm^{-1}): 2948 (Ar, C–H st), 1711, 1593 (pyrrole ring), 1500, 1276, 1199 (C–F st), 1132 (C–F st). MS (MALDI, matrix: DCTB) for $C_{108}H_{84}F_{24}N_{12}O_8Zn$: *m/z* [M] + [M+H]$^+$ mixture 2196.5 (calculated: 2196.5), 2151.4 (calculated: 2151.5) [M-($HNMe_2$)], 2106.3 (calculated: 2016.4) [M-2($HNMe_2$)]. Due to the large number of ions in the region of the molecular ion it is not possible to measure the exact mass reliably by possible interference with the internal standard.

PS-3: ZnPc **6** (10 mg, 4.4 x 10^{-3} mmol) was placed in a 5 mL high pressure resistant flask equipped with a magnetic stirrer and

0.9 mL of dry EtOH (dried over 4 Å molecular sieves) were added. Then, an excess of MeI (20 eq.) was added and the mixture was refluxed overnight. After cooling the solvent was removed under vacuum. The residue was washed with EtOAc and heptane and it was filtered off to obtain a green solid. Yield: 2 mg (19%). 250 mg of Dowex® (1x8 200–400) were suspended in 10 mL of MiliQ water, the product was previously dissolved in 0.2 mL of DMSO was added and stirred for 2 h. Then, the mixture was filtered, washed with diethylether, and evaporated under vacuum. ^{1}H NMR (500 MHz, DMSO-d_6): δ 2.25 (br s, 8H, CH_2), 3.14 (s, 36H, CH_3), 3.54 (m, 8H, CH_2), 4.10 (br s, 8H, CH_2), 6.85–7.17 (m, 16H, Ar), 7.76 (s, 4H, Ar), 7.98 (s, 4H, Ar), 8.24 (s, 4H, Ar), 8.77 (s, 8H, Ar). IR (ATR) ν^{-1} (cm^{-1}): 2929 (ar, C–H st), 1616 (pyrrole ring), 1501, 1277, 1196 (C–F st), 1133 (C–F st). HR-MS (ESI Positive TOF_MS-100-3500.m) for $C_{112}H_{96}F_{24}N_{12}O_8Zn$: *m/z* 763.8681 $[MCl]^{3+}$ (calculated: 763.8685); 1163.2876 $[MCl_2]^{2+}$ (calculated: 1163.2874).

Declaration of competing interest

The authors declare that they have no known competing financial interests or personal relationships that could have appeared to influence the work reported in this paper.

Acknowledgements

This work has been supported by MINECO, Spain (CTQ2017-85393-P and CTQ2016-78454-C2-1-R). C. H. thanks the European Social Funds and the SUR del DEC de la Generalitat de Catalunya for his predoctoral fellowships (Grant No. 2017 FI_B00617, 2018 FI_B1 00174 and 2019 FI_B2 00167).

Appendix A. Supplementary data

Supplementary data to this article can be found online at https://doi.org/10.1016/j.ejmech.2019.111957.

References

[1] D.E.J.G.J. Dolmans, D. Fukumura, R.K. Jain, Photodynamic therapy for cancer, Nat. Rev. Cancer 3 (2003) 380–387.
[2] M. Wainwright, T. Maisch, S. Nonell, K. Plaetzer, A. Almeida, G.P. Tegos, M.R. Hamblin, Photoantimicrobials—are we afraid of the light? The Lancet Infectious Diseases 17 (2) (2017) e49–e55, https://doi.org/10.1016/S1473-3099(16)30268-7.
[3] D.M.A. Vera, M.H. Haynes, A.R. Ball, T. Dai, C. Astrakas, M.J. Kelso, M.R. Hamblin, G.P. Tegos, Strategies to potentiate antimicrobial photoinactivation by overcoming resistant phenotypes, Photochem. Photobiol. 88 (2012) 499–511.
[4] M. Wainwright, Photodynamic antimicrobial chemotherapy (PACT), J. Antimicrob. Chemother. 42 (1998) 13–28.
[5] E. Alves, M.A.F. Faustino, M.G.P.M.S. Neves, A. Cunha, H. Nadais, A. Almeida, Potential applications of porphyrins in photodynamic inactivation beyond the medical scope, J. Photochem. Photobiol. C Photochem. Rev. 22 (2015) 34–57.
[6] R. Yin, T. Agrawal, U. Khan, G.K. Gupta, V. Rai, Y.-Y. Huang, M.R. Hamblin, Antimicrobial photodynamic inactivation in nanomedicine: small light strides against bad bugs, Nanomedicine 10 (2015) 2379–2404.
[7] B. Habermeyer, R. Guilard, Some activities of PorphyChem illustrated by the applications of porphyrinoids in PDT, PIT and PDI, Photochem. Photobiol. Sci. 17 (2018) 1675–1690.
[8] M.Q. Mesquita, C.J. Dias, M.G.P.M.S. Neves, A. Almeida, M.A.F. Faustino, Revisiting current photoactive materials for antimicrobial photodynamic therapy, Molecules 23 (2018) 1–47.
[9] V. Almeida-Marrero, E. van de Winckel, E. Anaya-Plaza, T. Torres, A. de la Escosura, Porphyrinoid biohybrid materials as an emerging toolbox for biomedical light management, Chem. Soc. Rev. 47 (2018) 7369–7400.
[10] X. Li, B.-D. Zheng, X.-H. Peng, S.-Z. Li, J.-W. Ying, Y. Zhao, J.-D. Huang, J. Yoon, Phthalocyanines as medicinal photosensitizers: developments in the last five years, Coord. Chem. Rev. 379 (2019) 147–160.
[11] Y. Li, J. Wang, X. Zhang, W. Guo, F. Li, M. Yu, X. Kong, W. Wu, Z. Hong, Highly water-soluble and tumor-targeted photosensitizers for photodynamic therapy, Org. Biomol. Chem. 13 (2015) 7681–7694.
[12] V. Koç, S.Z. Topal, D. Aydın Tekdaş, Ö.D. Ateş, E. Önal, F. Dumoulin, A.G. Gürek, V. Ahsen, Assessment of the relevance of GaPc substituted with azido-polyethylene glycol chains for photodynamic therapy. Design, synthetic strategy, fluorescence, singlet oxygen generation, and pH-dependent spectroscopic behaviour, New J. Chem. 41 (2017) 10027–10036.
[13] L.M.O. Lourenco, D.M.G.C. Rocha, C.I.V. Ramos, M.C. Gomes, A. Almeida, M.A.F. Faustino, F.A. Almeida Paz, M.G.P.M. S Neves, A. Cunha, J.P.C. Tome, Photoinactivation of planktonic and biofilm forms of Escherichia coli through the action of cationic zinc(II) Phthalocyanines, ChemPhotoChem 3 (2019) 251–260.
[14] U. Isci, M. Beyreis, N. Tortik, S.Z. Topal, M. Glueck, V. Ahsen, F. Dumoulin, T. Kiesslich, K. Plaetzer, Methylsulfonyl Zn phthalocyanine: a polyvalent and powerful hydrophobic photosensitizer with a wide spectrum of photodynamic applications, Photodiagn. Photodyn. 13 (2016) 40–47.
[15] L.M. Lourenco, A. Sousa, M.C. Gomes, M.A.F. Faustino, A. Almeida, A.M.S. Silva, M.G.P.M.S. Neves, J.A.S. Cavaleiro, A. Cunha, J.P.C. Tome, Inverted methoxypyridinium phthalocyanines for PDI of pathogenic bacteria, Photochem. Photobiol. Sci. 14 (2015) 1853–1863.
[16] M.B. Spesia, M. Rovera, E.N. Durantini, Photodynamic inactivation of Escherichia coli and Streptococcus mitis by cationic zinc(II) phthalocyanines in media with blood derivatives, Eur. J. Med. Chem. 45 (2010) 2198–2205.
[17] E. van de Winckel, B. David, M.M. Simoni, J.A. González-Delgado, A. de la Escosura, Â. Cunha, T. Torres, Octacationic and axially di-substituted silicon (IV) phthalocyanines for photodynamic inactivation of bacteria, Dyes Pigments 145 (2017) 239–245.
[18] A. Ullah, Y. Zhang, Z. Iqbal, Y. Zhang, D. Wang, J. Chen, P. Hu, Z. Chen, M. Huang, Household light source for potent photo-dynamic antimicrobial effect and wound healing in an infective animal model, Biomed. Opt. Express 9 (2018) 1006–1019.
[19] Y. Zhao, J.-W. Ying, Q. Sun, M.-R. Ke, B.-Y. Zheng, J.-D. Huang, A novel silicon(IV) phthalocyanine-oligopeptide conjugate as a highly efficient photosensitizer for photodynamic antimicrobial therapy, Dyes Pigments 172 (2020) 107834.
[20] A. Sindelo, N. Kobayashi, M. Kimura, T. Nyokong, Physicochemical and photodynamic antimicrobial chemotherapy activity of morpholine-substituted phthalocyanines: effect of point of substitution and central metal, J. Photochem. Photobiol. A Chem. 374 (2019) 58–67.
[21] X.F. Zhang, Q. Xi, J. Zhao, Fluorescent and triplet state photoactive J-type phthalocyanine nano assemblies: controlled formation and photosensitizing properties, J. Mater. Chem. 20 (2010) 6726–6733.
[22] E. Fazio, J. Jaramillo-García, G. de La Torre, T. Torres, Efficient synthesis of ABAB functionalized phthalocyanines, Org. Lett. 16 (2014) 4706–4709.
[23] E. Fazio, M.K. Nazeerudin, G. de la Torre, M. Medel, M. Grätzel, J. Jaramillo-García, M. Urbani, T. Torres, ABAB phthalocyanines: scaffolds for building unprecedented donor-π-acceptor chromophores, Chemistry 6 (2016) 121–127.
[24] M.A. Revuelta-Maza, C. Hally, S. Nonell, G. de la Torre, T. Torres, Crosswise phthalocyanines with collinear functionalization: new paradigmatic derivatives for efficient singlet oxygen photosensitization, ChemPlusChem 84 (2019) 673–679.
[25] M.A. Revuelta-Maza, S. Nonell, G. de la Torre, T. Torres, Boosting the singlet oxygen photosensitization abilities of Zn(II) phthalocyanines through functionalization with bulky fluorinated substituents Org, Biomol. Chem. 17 (2019) 7448–7454.
[26] W. Duan, P.C. Lo, L. Duan, W.P. Fong, D.K.P. Ng, Preparation and in vitro photodynamic activity of amphiphilic zinc(II) phthalocyanines substituted with 2-(dimethylamino)ethylthio moieties and their N-alkylated derivatives, Bioorg. Med. Chem. 18 (2010) 2672–2677.
[27] L.J. Campbell, L.F. Borges, F.J. Heldrich, Microwave accelerated preparation of aryl 2-(N,N-diethylamino)ethyl ethers, Bioorg. Med. Chem. Lett 4 (1994) 2627–2630.
[28] P. Abós, C. Artigas, S. Bertolotti, S.E. Braslavsky, P. Fors, K. Lang, S. Nonell, F.J. Rodríguez, M.L. Sesé, F.R. Trull, Polymer bound pyrrole compounds, IX. Photophysical and singlet molecular oxygen photosensitizing properties of mesoporphyrin IX covalently bound to a low molecular weight polyethylene glycol, J. Photochem. Photobiol. B Biol. 41 (1997) 53–59.
[29] R. Ezzeddine, A. Al-Banaw, A. Tovmasyan, J.D. Craik, I. Batinic-Haberle, L.T. Benov, Effect of molecular characteristics on cellular uptake, subcellular localization, and phototoxicity of Zn(II) N-alkylpyridylporphyrins, J. Biol. Chem. 288 (2013) 36579–36588.
[30] I.O.L. Bacellar, C. Pavani, E.M. Sales, R. Itri, M. Wainwright, M.S. Baptista, Membrane damage efficiency of phenothiazinium photosensitizers, Photochem. Photobiol. 90 (2014) 801–813.
[31] F.M. Engelmann, S.V.O. Rocha, H.E. Toma, K. Araki, M.S. Baptista, Determination of n-octanol/water partition and membrane binding of cationic porphyrins, Int. J. Pharm. 329 (2007) 12–18.
[32] L. Alonso, R.N. Sampaio, T.F.M. Souza, R.C. Silva, N.M.B. Neto, A.O. Ribeiro, A. Alonso, P.J. Gonçalves, Photodynamic evaluation of tetracarboxyphthalocyanines in model systems, J. Photochem. Photobiol. B Biol. 161 (2016) 100–107.
[33] X. Wang Wang, B. Zhang, Mitochondria-targeting properties and photodynamic activities of porphyrin derivatives bearing cationic pendant, J. Photochem. Photobiol. B Biol. 98 (2010) 167–171.
[34] X. Ragàs, X. He, M. Agut, M. Roxo-Rosa, R.A. Gonsalves, C.A. Serra, S. Nonell, Singlet oxygen in antimicrobial photodynamic therapy: photosensitizer-dependent production and decay in E. coli, Molecules 18 (2013) 2712–2725.
[35] X. Ragàs, M. Agut, S. Nonell, Singlet oxygen in Escherichia coli: new insights

for antimicrobial photodynamic therapy, Free Radic. Biol. Med. 49 (2010) 770–776.
[36] R. Yin, M.R. Hamblin, Antimicrobial photosensitizers: drug discovery under the spotligh, Curr. Med. Chem. 22 (2015) 2159–2185.
[37] R. Ruiz-González, M. Agut, E. Reddi, S. Nonell, A comparative study on two cationic porphycenes: photophysical and antimicrobial photoinactivation evaluation, Int. J. Mol. Sci. 16 (2015) 27072–27086.
[38] J.B. Pereira, E.F.A. Carvalho, M.A.F. Faustino, R. Fernandes, M.G.P.M.S. Neves, J.A.S. Cavaleiro, N.C.M. Gomes, Â. Cunha, A. Almeida, J.P.C. Tomé, Phthalocyanine thio-pyridinium derivatives as antibacterial photosensitizers, Photochem. Photobiol. 88 (2012) 537–547.
[39] E. Anaya-Plaza, E. van de Winckel, J. Mikkilä, J.-M. Malho, O. Ikkala, O. Gulías, R. Bresolí-Obach, M. Agut, S. Nonell, T. Torres, et al., Photoantimicrobial biohybrids by supramolecular immobilization of cationic phthalocyanines onto cellulose nanocrystals, Chem. Eur J. 23 (2017) 4320–4326.
[40] D.S. Terekhov, K.J.M. Nolan, C.R. McArthur, C.C. Leznoff, Synthesis of 2,3,9,10,16,17,23,24-octaalkynylphthalocyanines and the effects of concentration and temperature on their 1H-NMR spectra, J. Org. Chem. 61 (1996) 3034–3040.
[41] H. Li, T.J. Jensen, F.R. Fronczek, M.G.H. Vicente, Syntheses and properties of a series of cationic water-soluble phthalocyanines, J. Med. Chem. 51 (2008) 502–511.
[42] M. Li, E. Khoshdel, D.M. Haddleton, Synthesis of water soluble PEGylated (copper) phthalocyanines via Mitsunobu reaction and Cu(I)-catalysed azide–alkyne cycloaddition (CuAAC) “click” chemistry, Polym. Chem. 4 (2013) 4405–4411.
[43] P. Bonakdarzadeh, F. Topić, E. Kalenius, S. Bhowmik, S. Sato, M. Groessl, R. Knochenmuss, K. Rissanen, DOSY NMR, X-ray structural and ion-mobility mass spectrometric studies on electron-deficient and electron-rich M6L4 coordination cages, Inorg. Chem. 54 (2015) 6055–6061.
[44] F. Aricò, S. Evaristo, P. Tundo, Chemical behavior and reaction kinetics of sulfur and nitrogen half-mustard and iprit carbonate analogues, ACS Sustain. Chem. Eng. 1 (2013) 1319–1325.